Materials Physics and Mechanics 45 (2020) 31-37 Received: March 11, 2020

3D FINITE ELEMENT, CONNECTED WITH ORTHOGONAL FINITE FUNCTIONS, IN MODELING AND INVESTIGATION OF ELASTIC HOMOGENEOUS AND HETEROGENEOUS MATERIALS

V.L. Leontiev[1*], I.V. Efremenkov[2]

[1]Peter the Great St.Petersburg Polytechnic University, Polytekhnicheskaya 29, 195251, St. Petersburg

[2]Ulyanovsk State University, Lev Tolstoy 42. Ulyanovsk, 432000, Russian Federation Russia

*e-mail: leontiev_vl@spbstu.ru

Abstract. A novel 2D finite element (FE) associated with orthogonal finite functions (OFF, orthogonal splines) was developed for the ANSYS software and was tested early. The expansion of this method is presented here. The novel 3D FE, connected with 3D OFF is proposed for modeling and investigation of the stress-strain state of homogeneous and heterogeneous elastic bodies. The accuracy of the solutions obtained with this 3D FE is as high as for the classic ANSYS 3D FE. The developed 3D FE requires significantly less computational time; the winning of computational time increases with the amount of FE in a model.

Keywords: 3D finite element, homogeneous material, heterogeneous materials, orthogonal finite function, shape function

1. Introduction

A novel 2D finite element (FE) associated with orthogonal finite functions (OFF, orthogonal splines) was developed for the ANSYS software and was tested in [1]. The development of advanced discrete 3D models and finite element methods (FEM) is an actual direction in computational mechanics, because it makes possible to explore technical structures with minimal simplifications of their geometry. This possibility is dictated by the properties of the 3D model and 3D FEM, which are characterized by lower computational time, compared to the classical 3D model and FEM, together with high accuracy of approximate solutions.

It is known that compactly supported orthonormal wavelets [2] have shown low efficiency in the finite element methods. The orthogonal splines [3], created specifically for the algorithms of variational-grid methods, finite element methods, have advantages before the wavelets [2]. The novel 3D FE for the ANSYS software is constructed on the basis of orthogonal splines [3]. The analysis of numerical results obtained for the 3D problem of elasticity shown that the application of the orthogonal splines in the 3D finite elements provides high accuracy of approximate solutions; besides the solution requires much less computational time in comparison with the classical 3D finite element. The orthogonal splines [3] remove main disadvantages of the mixed-finite-element methods, which produce approximate solutions for strains and stresses without numerical differentiation [3-7]. However, in a complex of program, such as ANSYS, the mixed-finite-element methods are not used.

http://dx.doi.org/10.18720/MPM.4512020_4

In this paper, it is illustrated, by the example of 3D elasticity problems, that the application of orthogonal splines in 3D finite elements for the FEM of ANSYS connected with the Lagrange's variational principle saves high accuracy of approximate solutions and significantly decreases the computational time.

2. 3D finite element connected with orthogonal splines

The novel FE, is similar to the FE Solid185 of ANSYS, has been constructed. The local stiffness matrix, the vector of body forces and loads on a boundary are created for the domain of FE – the parallelepiped. The eight nodes of the base 3D finite element have the following numbers and coordinates**: 1** (-1,-1,1), **2** (-1,1,1), **3** (-1,-1,-1), **4** (-1,1,-1), **5** (1,1,-1), **6** (1,-1,-1), **7** (1,1,1), **8** (1,-1,1).

The system of equations of 3D linear elasticity can be written in a matrix form [1]:

$$\varepsilon = Bu,\ \sigma = D\varepsilon,\ B^T\sigma = f. \quad (1)$$

However the displacement vector, the strain vector, the stress vector, the vector of body forces has other structure:

$u = (u_1, u_2, u_3)^T,\ \ \varepsilon = (\varepsilon_{11}, \varepsilon_{22}, \varepsilon_{33}, \varepsilon_{12}, \varepsilon_{23}. \varepsilon_{31})^T,$

$\sigma = (\sigma_{11}, \sigma_{22}, \sigma_{33}, \sigma_{12}, \sigma_{23}. \sigma_{31})^T,\ f = (f_1, f_2, f_3)^T.$

Here D is the known matrix (6×6) of elastic modules; B is the known matrix differential operator (6×3).

$$u_j(x,y,z) = \sum_{i=1}^{8} N_i(x,y,z)u_j^i\ ,\ \ (j = 1,2,3) \quad (2)$$

in the domain of 3D finite element, u_j^i are unknown constant coefficients; $N_i(x,y,z)$ are the shape functions, which have the property: $N_i(x_j, y_j, z_j) = \delta_{ij},$ of the Lagrange's basis on a 3D finite element.

3D problem (1) after discretization (2) and exception of ε and σ can be written in the form similar to [1]:

$$KU = f,\ \ K = \sum_{(e)} k^{(e)},\ \ \ f = \sum_{(e)} f^{(e)},$$

where the global stiffness matrix K and unknown vector U have other structure by comparison with [1], U is the global vector of unknown displacements in the nodes of a 3D grid. The local stiffness matrix $k^{(e)}$ and the local vector $f^{(e)}$ of body forces and loads on the boundary $S^{(e)}$ of the FE are written as in [1]:

$$k^{(e)} = \int_{V^{(e)}} B^T DB dV,\ f^{(e)} = \int_{V^{(e)}} N^T f dV + \int_{S^{(e)}} N^T p dS\ , \quad (3)$$

however they are defined by other known operators B, D and by another matrix N of the shape functions.

Here $p = (p_1, p_2, p_3)$ – the vector of a load on the boundary $S^{(e)}$ of the region $V^{(e)}$. Formulas (3) were used for construction of the novel finite element method of 3D linear elasticity theory connected with orthogonal splines, including the corresponding subroutines for ANSYS. The subroutines define operations with functions (4), the matrices of novel 3D finite element, and output of numerical solutions.

The shape functions for the rectangular parallelepiped of novel FE are

$$N_i(\xi,\eta,\zeta) = \varphi_i(\xi)\varphi_i(\eta)\varphi_i(\zeta),\ \ (i = \overline{1,8})\ , \quad (4)$$

they are defined by Table 1, where ξ, η, ζ – the local coordinates of 3D finite element.

The OFFs [1,3]

$$\psi_1(\mu) = \begin{cases} \dfrac{(\sqrt{2}-1)(\mu+1)}{2} + 1,\ \ \mu \in [-1,0]; \\ \dfrac{(\sqrt{2}+1)(1-\mu)}{2},\ \ \mu \in [0,1\,]; \end{cases} \quad \psi_2(\mu) = \begin{cases} \dfrac{(1-\sqrt{2})(1+\mu)}{2},\ \ \mu \in [-1,0]; \\ \dfrac{(\sqrt{2}+1)(\mu-1)}{2} + 1,\ \ \mu \in [0,1]; \end{cases}$$

have the properties

$\psi_1(-1) = 1,\ \psi_1(0) = (\sqrt{2}+1)/2,\ \psi_1(1) = 0;$

$\psi_2(-1) = 0,\ \psi_2(0) = (1-\sqrt{2})/2,\ \psi_2(1) = 1$

of Lagrange's basis on [-1, 1]. These functions are finite and orthogonal on [-1, 1] with weight equal to 1. The functions $\psi_1(\mu)$, $\psi_2(\mu)$ define 1D orthogonal splines $\varphi_i(\xi)$, $\varphi_i(\eta)$, $\varphi_i(\zeta)$ and 3D orthogonal finite functions N_i in Table 1.

Table 1. 1D orthogonal splines for the functions (4)

N_1	$\varphi_1(\xi) = \psi_1(\xi)$ $\varphi_1(\eta) = \psi_1(\eta)$ $\varphi_1(\zeta) = \psi_2(\zeta)$	N_5	$\varphi_5(\xi) = \psi_2(\xi)$ $\varphi_5(\eta) = \psi_2(\eta)$ $\varphi_5(\zeta) = \psi_1(\zeta)$
N_2	$\varphi_2(\xi) = \psi_1(\xi)$ $\varphi_2(\eta) = \psi_2(\eta)$ $\varphi_2(\zeta) = \psi_2(\zeta)$	N_6	$\varphi_6(\xi) = \psi_2(\xi)$ $\varphi_6(\eta) = \psi_1(\eta)$ $\varphi_6(\zeta) = \psi_1(\zeta)$
N_3	$\varphi_3(\xi) = \psi_1(\xi)$ $\varphi_3(\eta) = \psi_1(\eta)$ $\varphi_3(\zeta) = \psi_1(\zeta)$	N_7	$\varphi_7(\xi) = \psi_2(\xi)$ $\varphi_7(\eta) = \psi_2(\eta)$ $\varphi_7(\zeta) = \psi_2(\zeta)$
N_4	$\varphi_4(\xi) = \psi_1(\xi)$ $\varphi_4(\eta) = \psi_2(\eta)$ $\varphi_4(\zeta) = \psi_1(\zeta)$	N_8	$\varphi_8(\xi) = \psi_2(\xi)$ $\varphi_8(\eta) = \psi_1(\eta)$ $\varphi_8(\zeta) = \psi_2(\zeta)$

The subroutine for calculation of the functions (4) is done through the use of Fortran77.

3. Solutions of the problems of 3D linear elasticity theory

Numerical solutions of 3D problems of linear elasticity theory were obtained using the classical and created novel finite elements of ANSYS.

Problem 1. The square face of a cubic body ($y = -1$) is rigidly fixed, the uniform pressure p_y=25000 *Pa* being applied to the body surface with the coordinate y=1, on four square faces ($x = -1$; $x = 1$, $z = -1$, $z = 1$) of the cubic body kinematics and force factors are not defined (Fig. 1). The symmetry center of the cubic body of size 2 *m* is the origin of coordinates. The Young's modulus of homogeneous isotropic material has the value 200 *GPa*, the Poisson's coefficient has the value 0.33.

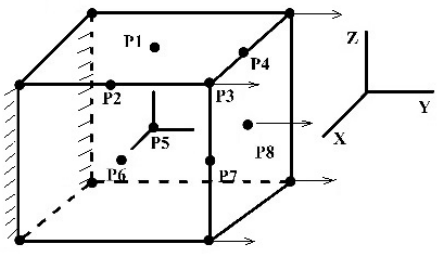

Fig. 1. Homogeneous cubic body

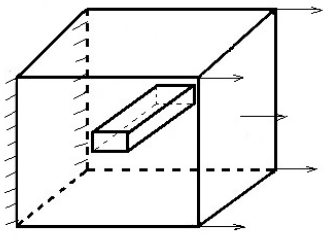

Fig. 2. Heterogeneous cubic body

Approximate solutions of this problem were obtained for different numbers *M* of FE divisions of every edge of the cube, ranging from 10 to 100 (the total number of FEs ranges from 1000 to 1000000). The results are given in Tables 2-8 for the points shown in Fig. 1. Points *P*1(0,0,1), *P*6(1,0 0) are in the centers of two faces of the cubic body. Point *P*8(0,1,0) is in the center of the body face, to which the uniform pressure $p = (p_x, p_y, p_z) = (0,25000,0)$

is applied. Points $P2(1,0,1)$, $P4(0,1,1)$, $P7(1,1,0)$ coincide with the middle of boundary edges of the cubic body. Point $P3(1,1,1)$ is in the cube vertex, point $P5(0,0,0)$ coincides with the origin of coordinates.

The calculation time [*ms*] in the finite element methods, employing User3D (t_1 [*ms*]) or Solid185 (t_2 [*ms*]) for the different values M, and the ratio $k=t_2/t_1$ are given in Table 2. The quantity k is the ratio of computational times of two FEMs. It increases with the rise of total number of FE due to the zero elements in the global grid matrix produced by OFFs. The values of k are larger in the 3D case in comparison with those in the 2D case [1]. The numerical results show that the created 3D finite element is characterized by lower computational time compared to the classical 3D model maintaining high accuracy of finite element solutions, and show higher efficiency of the application of orthogonal splines in 3D FEM in comparison with 2D FEM [1].

Table 2. The ratio of computational times of two FEMs

M	t_1	t_2	k
50	47	119	2.6
60	76	201	2.7
70	160	486	3.0
80	311	1015	3.3
90	583	1969	3.4
100	1009	3691	3.7

Table 3. The displacements in points $P1$, $P6$ of the homogeneous body and the relative differences

M	$10^7 U_{3D}$	$10^7 U_{185}$	$10^3 \varepsilon_1$	$10^2 \varepsilon_2$
50	1.23636	1.23628	6.28	2.58
60	1.23648	1.23642	4.89	1.57
70	1.23656	1.23652	3.49	0.939
80	1.23661	1.23659	2.09	0.525
90	1.23665	1.23664	0.693	0.250
100	1.23667	1.23668	0.263	0.026

Table 4. The displacements in point $P2$ of the homogeneous body and the relative differences

M	$10^7 U_{3D}$	$10^7 U_{185}$	$10^3 \varepsilon_1$	$10^2 \varepsilon_2$
50	1.34838	1.34829	6.61	1.93
60	1.34849	1.34842	5.23	1.16
70	1.34855	1.34850	3.81	0.681
80	1.34859	1.34856	2.43	0.366
90	1.34862	1.34861	1.05	0.161
100	1.34864	1.34864	0.246	0.025

Table 5. The displacements in point *P*3 of the homogeneous body and the relative differences

M	$10^7 U_{3D}$	$10^7 U_{185}$	$10^3 \varepsilon_1$	$10^2 \varepsilon_2$
50	2.50457	2.50440	6.75	1.12
60	2.50470	2.50456	5.35	0.607
70	2.50477	2.50467	3.96	0.313
80	2.50481	2.50475	2.54	0.148
90	2.50483	2.50481	1.14	0.060
100	2.50484	2.50485	0.258	0.026

Table 6. The displacements in points *P*4, *P*7 of the homogeneous body and the relative differences

M	$10^7 U_{3D}$	$10^7 U_{185}$	$10^3 \varepsilon_1$	$10^2 \varepsilon_2$
50	2.44589	2.44574	6.19	1.01
60	2.44600	2.44588	4.81	0.568
70	2.44606	2.44598	3.40	0.318
80	2.44609	2.44605	2.00	0.175
90	2.44611	2.44610	0.626	0.101
100	2.44613	2.44614	0.285	0.029

Table 7. The displacements in point *P*5 of the homogeneous body and the relative differences

M	$10^7 U_{3D}$	$10^7 U_{185}$	$10^3 \varepsilon_1$	$10^2 \varepsilon_2$
50	1.11088	1.11081	6.34	3.52
60	1.11103	1.11097	4.94	2.15
70	1.11112	1.11108	3.55	1.29
80	1.11119	1.11116	2.13	0.716
90	1.11123	1.11122	0.725	0.330
100	1.11126	1.11127	0.313	0.031

Table 8. The displacements in point *P*8 of the homogeneous body and the relative differences

M	$10^7 U_{3D}$	$10^7 U_{185}$	$10^3 \varepsilon_1$	$10^2 \varepsilon_2$
50	2.39363	2.39349	6.01	1.09
60	2.39374	2.39363	4.62	0.638
70	2.39381	2.39373	3.21	0.370
80	2.39384	2.39380	1.81	0.215
90	2.39386	2.39385	0.420	0.131
100	2.39389	2.39390	0.253	0.025

The values ($10^7 U_{3D}$) [m] and ($10^7 U_{185}$) [m] of the module of displacement vector for specified points of the cubic body are given in Tables 3-8. These results were produced by two methods, which use finite elements User3D and Solid185. Tables 3-8 have also two values**:** ε_1 [%] – the relative difference of two solutions obtained on the specified grid and ε_2 [%] – the relative difference of the User3D approximation for the specified *M* and the Solid185 approximation for maximal *M* (*M*=100, 1000000 FE). The result obtained with the help of Solid185 finite element for maximal *M* is considered to be a benchmark solution, because an additional increase of *M* gives little variations of the solutions.

Comparison of the solution U_{3D}, obtained using the finite element User3D connected with orthogonal splines, and finite element solution U_{185} produced by classical FEM of ANSYS shows high-precision of U_{3D}; it is confirmed by the relative difference ε_1. The decrease of the relative difference ε_2 demonstrates the high accuracy of the solutions U_{3D} on the employed grids.

Problem 2. A heterogeneous cubic body has the sizes and properties of the main region of Problem 1. However the region $(-1 \le x \le 1;\ -0.2 \le y \le 0.2; -0.1 \le z \le 0.1)$ of the body (Fig. 2) possesses other properties**:** the Young's modulus being equal to 160 *GPa*, and the Poisson's coefficient has the value 0.3. The boundary conditions are the same as in Problem 1.

From Tables 9-11 it follows that the numerical results both for the heterogeneous elastic body and for the homogeneous body are similar. The finite element method, connected with orthogonal splines, demonstrates a high-precision of finite element results U_{3D} and reduced computational time in Problems 1 and 2. Thereby, the FE models with orthogonal splines are effective for solving 3D problems for homogeneous and heterogeneous elastic materials.

Table 9. The displacements in point *P*1 of the heterogeneous body and the relative differences

M	$10^7 U_{3D}$	$10^7 U_{185}$	$10^3 \varepsilon_1$	$10^2 \varepsilon_2$
50	1.23945	1.23937	6.18	2.60
60	1.23953	1.23947	4.42	1.99
70	1.23956	1.23953	2.81	1.70
80	1.23960	1.23959	1.19	1.36
90	1.23967	1.23967	0.421	0.859
100	1.23977	1.23977	0.387	0.039

Table 10.The displacements in point *P*2 of the heterogeneous body and the relative differences

M	$10^7 U_{3D}$	$10^7 U_{185}$	$10^3 \varepsilon_1$	$10^2 \varepsilon_2$
50	1.35150	1.35143	5.24	2.08
60	1.35164	1.35159	3.82	1.05
70	1.35169	1.35165	2.56	0.711
80	1.35172	1.35171	1.29	0.446
90	1.35175	1.35174	0.766	0.233
100	1.35178	1.35178	0.322	0.032

Table 11. The displacements in point *P*8 of the heterogeneous body and the relative differences

M	$10^7 U_{3D}$	$10^7 U_{185}$	$10^3 \varepsilon_1$	$10^2 \varepsilon_2$
50	2.40319	2.40302	7.02	0.642
60	2.40326	2.40313	5.34	0.372
70	2.40327	2.40317	4.08	0.303
80	2.40329	2.40321	3.23	0.243
90	2.40333	2.40329	1.84	0.068
100	2.40334	2.40335	0.228	0.023

Problems for 3D elastic bodies with several small regions, which have different properties, were solved also. The accuracy of these numerical results and the quantities of computational time were found to be similar to such parameters of the solutions of the Problems 1, 2.

The author created theoretical foundations and the algorithm for forming of novel finite 2D, 3D elements connected with OFF. The coauthor carried out programming of these finite elements and produced calculations.

Conclusions

A novel 2D FE, connected with 2D OFF, was developed for ANSYS software and was tested in [1]. Here the development of the method [1] is presented. A novel 3D FE, connected with 3D orthogonal splines, is proposed for modeling and investigation of homogeneous and heterogeneous elastic 3D bodies. It is shown that the novel 3D finite element method with orthogonal splines is effective. This FEM gives high-precision finite element solutions U_{3D} with reduced computational time. The calculation results demonstrate that orthogonal splines allow not only to improve the characteristics of mixed FEMs, but also of classical FEMs based on the Lagrange's variational principle, which form the basis of ANSYS.

Acknowledgements. *No external funding was received for this study.*

References

[1] Leontiev VL, Efremenkov IV. Finite element modeling and investigation of elastic homogeneous and heterogeneous materials. *Materials Physics and Mechanics.* 2019;42(3): 340-350.

[2] Daubechies I. Orthonormal bases of compactly supported wavelets. *Comm. Pure and Appl. Math.* 1988;41(7): 909-996.

[3] Leontiev VL. *Orthogonal Finite Functions and Numerical Methods.* Ulyanovsk: UlGU; 2003. (In Russian)

[4] Ciarlet P. *The Finite Element Method for Elliptic Problems.* Amsterdam: North-Holland Publ. Comp.; 1978.

[5] Poceski A. *Mixed Finite Element Method.* Berlin: Springer; 1992.

[6] Brezzi F, Douglas J, Marini LD. Two Families of Mixed Finite Elements for Second Order Elliptic Problems. *Numer. Math.* 1985;47: 217-235.

[7] Boffi D, Brezzi F, Fortin M. *Mixed Finite Element Methods and Applications*. Springer Series in Computational Mathematics. Vol. 44. Springer; 2013.